

Surface Pressure Loading Technology of Ship Structures

DAI Ze-yu^{1,2}, WEI Peng-yu^{1,2}, CHEN Xiao-ping^{1,2}, JIANG Ze^{1,2}, CHEN Zhe^{1,2}, TANG Qin³

(1. China Ship Scientific Research Center, Wuxi 214082, China; 2. Taihu Laboratory of Deepsea Technological Science, Wuxi 214082, China; 3. School of Foreign Studies, Jiangnan University, Wuxi 214122, China)

Abstract: A hull structure is prone to local deformation and damage due to the pressure load on the surface. How to simulate surface pressure is an important issue in ship structure test. The loading mode of hydraulic actuator combined with high-pressure flexible bladder was proposed, and the numerical model of the loading device based on flexible bladder was established. The design and analysis method of high-pressure flexible bladder based on aramid-fiber reinforced thermoplastic polyurethane was proposed to break through the surface pressure loading technology of ship structures. The surface pressure loading system based on flexible bladder was developed. The ultimate strength verification test of the box girder under the combined action of bending moment and pressure was carried out to systematically verify the feasibility and applicability of the loading system. The results show that the surface pressure loading technology can be used well for applying uniform pressure to ship structures. Compared with the traditional surface loading methods, the improved device can be applied with horizontal constant pressure load, with rapid response and safe process, and the pressure load is always stable with the increase of the bending moment load during the test. The requirement for uniform loading in the comprehensive strength test of large structural models is satisfied and the accuracy of the test results is improved by this system.

Key words: surface pressure load; loading system; ship structure; strength test; flexible bladder

CLC number: U661.1 **Document code:** A **doi:** 10.3969/j.issn.1007-7294.2024.12.010

0 Introduction

During actual navigation, a hull structure is subjected to many different types of surface loads, such as outboard water pressure caused by wave load, local pressure caused by wind load and slamming load, and cargo pressure caused by pitching and heaving. In order to truly simulate the bearing characteristics and response results of hull structures under surface pressure load, surface pressure simulation and loading technology is particularly important.

At present, the uniform loading simulation methods used in the strength test of hull structure mainly include: piled-load loading method, tension/compression pad loading method and airbag loading method, as shown in Fig.1. The principle of piled-load loading method is simple, but the loading mode is not flexible enough. Since this method depends on the gravity of sandbags, iron

Received date: 2024-06-21

Foundation item: Supported by the National Key Research and Development Program of China (2022YFB3404800)

Biography: DAI Ze-yu(1995-), male, engineer, E-mail: daizeyujob@163.com; WEI Peng-yu(1982-), male, professor.

blocks, etc., it is suitable only for vertical loading with small loading levels, and manual loading and unloading is required in this method.^[1-2] The loading system of the tension/compression pad loading method is utilized to equivalently discretize the concentrated load provided by the actuator to several loading points^[3-5]. The method of adding loading pad has the advantages of fast loading acceleration and good flexibility. However, most ship structural parts are curved surfaces, so the directions of force lines between different loading points are different plane straight lines, which makes it difficult for the lever to achieve balance during loading. Moreover, during the test, the load direction of the loading point will change due to the deformation of the structure, thus affecting the accuracy of the test loading. Airbag loading method can realize uniform loading by controlling the pressure difference inside and outside the airbag, and has been successfully applied to aviation and civil engineering^[6-7]. Wang et al^[8] and Yang et al^[9] demonstrated the feasibility of uniformly distributed load applied by airbags in aircraft structural tests. Padalu et al^[10] applied uniform lateral pressure to the side of the wall by air bag loading. Shanmugam et al^[11] used an actuator to push the airbag to apply a combined axial compression and surface pressure load on the stiffened plate. Because the ship structural model is large in scale and bears a great local load, it is not mature to carry out strength test on the hull by airbag loading method at present. Moreover, sharp objects or high loads on the surface of a test structure may cause serious air leakage or even explosion of the airbag, which makes it difficult to ensure the safety of the test.



(a) Piled-load loading method



(b) Tension/compression pad loading method



(c) Airbag loading method



Fig.1 Typical methods of surface pressure loading

Therefore, in order to overcome the shortcomings of the above-mentioned typical surface pressure loading methods, an improved surface pressure loading method for ship structures is proposed and explored. By developing the design method of high-pressure flexible bladder based on aramid fiber reinforced thermoplastic polyurethane, the evaluation method of surface loading uniformity is established, and the surface pressure loading technology of ship structure test is explored. Moreover, the surface pressure loading system based on high-pressure flexible bladder is developed, and

the feasibility of uniform pressure loading is verified by model test. The related technology can serve as an important reference for the test load application of complex hull structure.

1 Design and analysis method of high-pressure flexible bladder

1.1 Loading mode of uniform pressure on ship structure surface

Hull structures are mostly curved structures and bear large external loads. In order to meet the requirements of uniform pressure loading on the surface of ship structure in strength test, a loading mode of hydraulic actuator combined with high-pressure flexible bladder is proposed, as shown in Fig.2. The flexible bladder is embedded in the rigid force transmission structure by bonding the support frame on the outside of the high-pressure flexible bladder. By pushing the rigid load transfer structure through the hydraulic actuator, the concentrated load from the actuator is converted into the internal pressure of the flexible bladder. The bladder pressure is finally evenly transmitted to the hull beam.

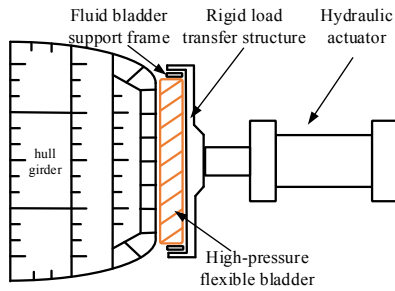


Fig.2 Diagram of loading mode

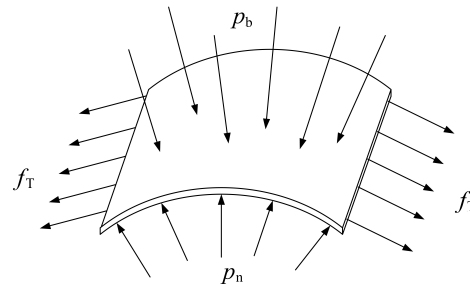


Fig.3 Schematic diagram of force analysis on the bladder skin unit

With the skin unit attached to the outer surface of the ship taken as the research object, the force analysis of the bladder skin unit is analyzed, as shown in Fig.3. According to the force balance,

$$(p_n - p_b) dS + f_T t ds = 0 \tag{1}$$

where, p_b is the pressure difference of bladder, and the direction is along the outer normal of the bladder surface; p_n is the load applied to the hull structure; f_T is the skin tension, the direction of which is tangential to the surface of bladder; S and s are the skin surface area and skin boundary, respectively; and t is the skin thickness.

The following equation is obtained by integrating Eq.(1):

$$\iint_S (p_n - p_b) dS + \oint_s f_T t ds = 0 \tag{2}$$

When the curvature of the loading surface is small, the loading surface can be approximated as a plane, then Eq.(2) can be simplified as

$$(p_n - p_b) \cdot S + f_T \cdot t \cdot c \cdot \sin\theta = 0 \tag{3}$$

where, c is the perimeter of the skin boundary, and when the curvature θ approaches 0, p_n can be obtained:

$$p_n = p_b \tag{4}$$

Therefore, the uniform loading on the surface of the hull structure can be achieved by changing the internal pressure p_b of the bladder.

1.2 Design of high-pressure flexible bladder

The high-pressure flexible bladder skin is made of aramid-fiber reinforced thermoplastic polyurethane polymer composite. Compared with neoprene, nylon and other materials, aramid-fiber has low initial modulus and good extensibility, which is beneficial for the bladder to transfer pressure to the hull structure during the initial loading stage. Moreover, the aramid-fiber has good corrosion resistance and high tensile strength, and the tensile strength can reach above 150 MPa. By covering the upper and lower surfaces of aramid-fiber with thermoplastic polyurethane, the oil resistance and wear resistance of the material are improved, providing excellent sealing performance for the bladder (see Fig.4).

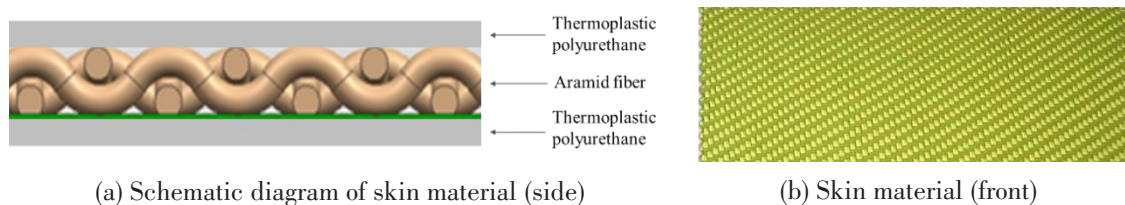


Fig.4 Bladder skin material

In order to simulate the hydrostatic pressure load on the bottom of the ship at the water depth of 10 m (corresponding to 100 kPa), the size of the bladder is designed as 1920 mm×2400 mm×100 mm, and the thickness is 3 mm. During skin welding, a high-frequency vibration wave of 20 kHz is transmitted to the skin joint. Heat is generated between the molecular chains on the skin surface, which fuses the cross section at the joint. Pressure is applied to complete ultrasonic welding.

1.3 Numerical simulation and verification

1.3.1 Mechanical properties of bladder skin materials

In order to accurately evaluate the uniformity of surface pressure loading, the tensile mechanical properties of the bladder skin are tested, as shown in Fig.5. A total of six specimens are prepared according to GB/T3354-2014 "Test Method for Tensile Properties of Orientation Fiber Reinforced Polymer Matrix Composite Materials". Each specimen is 250 mm in length, 25 mm in width, and 3 mm in thickness. The No. 6# specimen is used as temperature compensation.

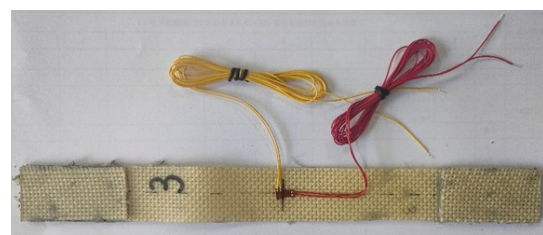


Fig.5 Tensile specimen of bladder skin

To obtain the longitudinal strain of the specimen during the tensile process, a resistance strain gauge is attached to the middle position of each specimen, and a 10 kN electronic universal testing machine is used to carry out the tensile strength test on the bladder skin. The specific test process is shown in Fig.6(a), and the failure morphology of the specimen is shown in Fig.6(b). It can be seen that when the surface layer fails, the inner aramid fiber bundle undergoes significant out-of-plane deformation and the edge fibers are pulled off. However, the thermoplastic polyurethane has not been torn and still maintains good sealing performance.



(a) Tensile strength test of bladder skin (b) Failure morphology of bladder skin

Fig.6 Failure morphology of bladder skin tensile specimen

According to the tensile stress–strain curves shown in Fig.7, the slope of the material tension curve increases at the initial stage as the bladder skin is gradually tightened (longitudinal strain is 0~0.03 ϵ), and the relationship between tensile stress and strain is approximately linear. With the increase of the load, the specimen exhibits out-of-plane deformation with the sound of fiber fracture, and the curve drops rapidly. Finally, the specimen loses its bearing capacity. The brittle failure characteristics are shown in the surface of the material. So, the elastic–brittle model is used to characterize the bladder skin, in which the tensile strength σ_b of No.2# specimen is the smallest, 167.0 MPa.

According to GB/T3354–2014, the elasticity modulus of the material is calculated by taking the stress–strain data of the bladder skin with the longitudinal strain ϵ in the range of 0.001~0.003 ϵ . The slope of the curve is obtained by using linear regression method. Taking No.3# specimen as the example, the elasticity modulus E of the aramid–fiber reinforced thermoplastic polyurethane polymer composite material is fitted to be 4.76 GPa, as shown in Fig.8.

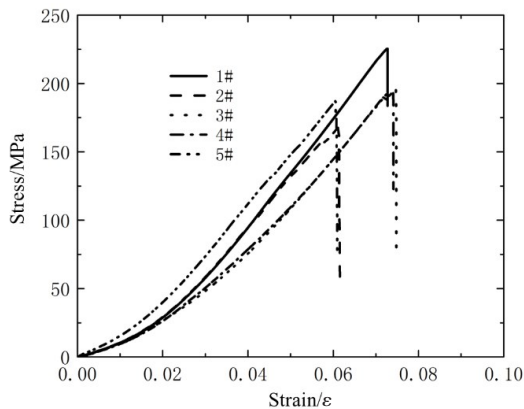


Fig.7 Stress–strain curve of bladder skin

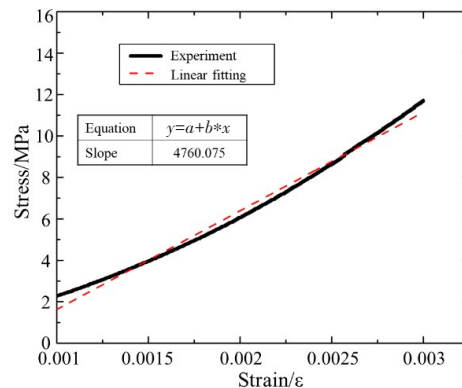


Fig.8 Fitting of elasticity modulus curve

1.3.2 Numerical simulation of loading device

The nonlinear finite element software ABAQUS is used to simulate the uniform load applied by bladder on the surface of ship structure. In order to accurately simulate the stress distribution and pressure application of bladder skin during the test, the finite element models of rigid load transfer structure, support frame, high–pressure flexible bladder and hull surface (replaced by rigid surface) are established respectively, as shown in Fig.9.

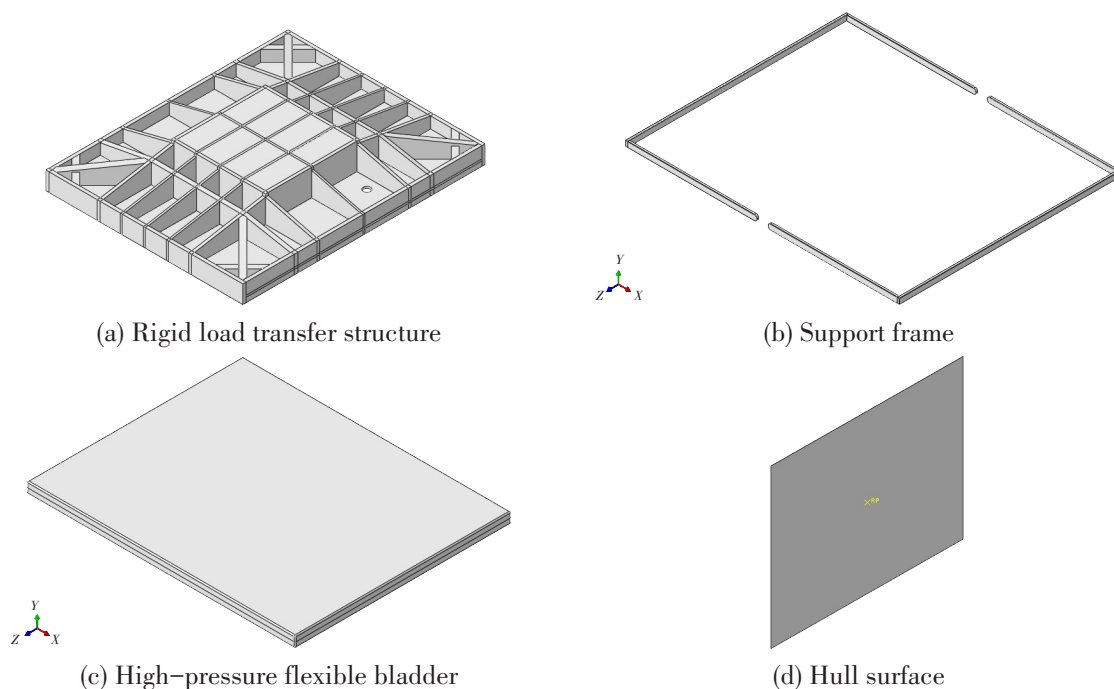


Fig.9 Finite element models

According to the tensile strength test results, the bladder skin is considered as an elastic–brittle model with a density of 1330 kg/m^3 . The elasticity modulus is 4.76 GPa , the Poisson’s ratio is 0.45 , and the minimum tensile strength is 167.0 MPa . The bladder is simulated by 4–node reduced integral shell element S4R. In order to avoid stress concentration, the boundary area between the high–pressure flexible bladder and the support frame is chamfered. To simulate the flow effect of squeezed hydraulic oil inside the bladder, the internal area of the bladder is set as a cavity, which is described by the fluid cavity function. The specific ambient pressure is the standard atmospheric pressure (101.36 kPa), the hydraulic oil density is set to 850 kg/m^3 , and the volume modulus is 1400 MPa .

The hull surface is replaced by a rigid surface, which is connected to the central reference point *A* through coupling constraints. The reference point *A* and the nodes at the back of the rigid load transfer structure are completely fixed, as shown in Fig.10. Tie connections are set between the support frame and the bladder or the support frame and the rigid load transfer structure. Contacts are set between the bladder and the rigid load transfer structure or the bladder and the hull. Due to the use of thermoplastic polyurethane as the bladder skin, the friction coefficient is taken as 0.18 .

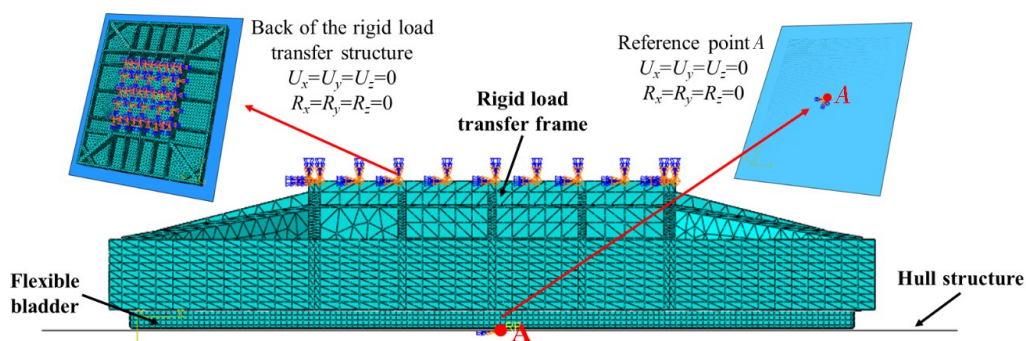


Fig.10 Numerical model of rigid load transfer structure–flexible bladder–hull structure

1.3.3 Simulation and verification of loading effect

As shown in Fig.11, the influence of the distance between the bladder and the hull on the loading effect is emphatically analyzed. At the initial stage of loading, there is a certain distance between the bladder and the rigid surface of the hull structure. The initial distance is selected as 5 mm, 8 mm and 11 mm in turn. The pressure of the bladder is slowly increased to 100 kPa, so as to ensure full contact between the bladder and the hull surface. The results show that the loading value is closest to the expected value when the distance between the bladder and the hull is 5 mm. With the increase of distance, the total load decreases gradually. Therefore, before the test begins, the distance between the bladder and the hull should be set as small as possible.

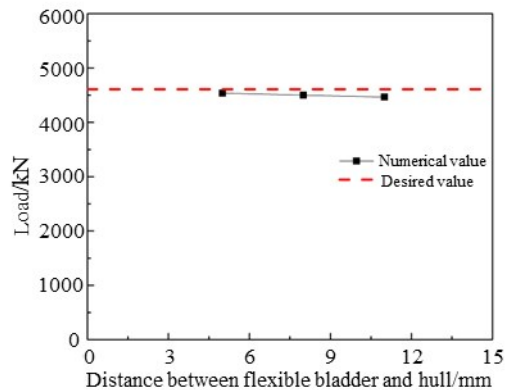
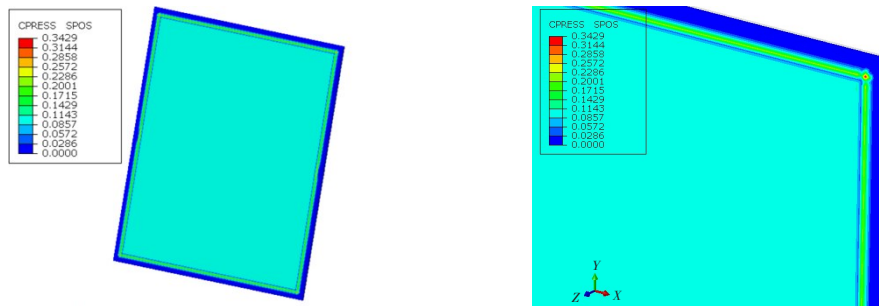


Fig.11 Comparison of load at different initial distances between the bladder and the hull

When the distance between the bladder and hull is 5 mm, the pressure distributions on the contact surface of the bladder are presented in Figs.12–13. It can be seen that the normal pressure on the contact surface is close to uniform distribution except for the high contact pressure at the outer edge of the bladder, achieving a uniform load of 100 kPa.

The distribution of in-plane principal stress on the surface of the bladder is shown in Fig.14.



(a) Normal pressure at contact surface (b) Peak pressure on the contact surface

Fig.12 Normal pressure of the contact surface between the bladder and the hull

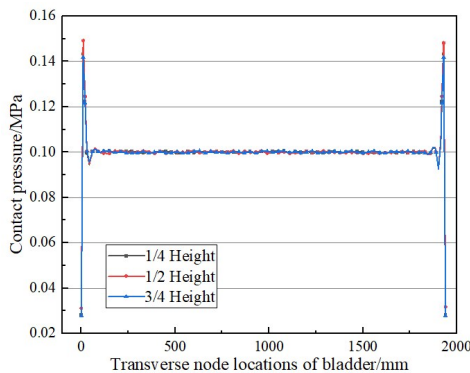


Fig.13 Pressure distribution of transverse nodes

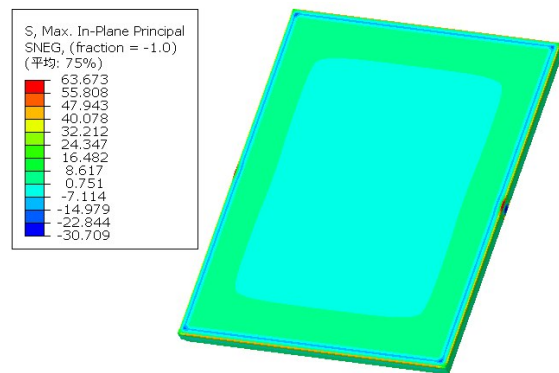


Fig.14 In-plane principal stress distribution

The in-plane principal stress level in the loading area of the bladder is small, no more than 10 MPa, while the high-stress area is mainly concentrated in the gap between the middle of the support frame and bladder. The maximum in-plane principal stress S_{\max} is 63.67 MPa. It can be seen from the upper section that the tensile strength of the bladder skin is $\sigma_b > S_{\max}$, therefore meeting the strength requirements.

2 Development of surface pressure loading system based on flexible bladder

The improved surface pressure loading system consists of a reaction device, a hydraulic actuator, a high-pressure flexible bladder (including support frame), a rigid load transfer structure and a liquid pressure sensor, as shown in Fig.15. The loading system can accurately simulate the hydrostatic pressure on the hull surface at a depth of 10 m. The main technical parameters of the system are as follows:

- (1) Loading area: 2400 mm×1920 mm (4.608 m²);
- (2) Design load: 100 kPa;
- (3) Maximum stroke: 500 mm.

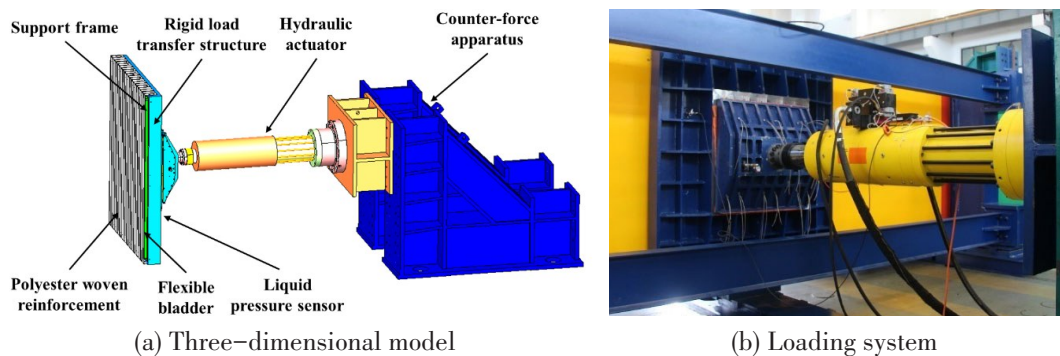


Fig.15 Surface pressure loading system

2.1 Hydraulic actuator

To achieve a uniform pressure of 100 kPa on the 4.608 m² loading area, the hydraulic actuator needs to provide a test load of at least 460.8 kN. Considering the design margin of load, a hydraulic servo actuator with a maximum stroke of 500 mm is selected.

2.2 High-pressure flexible bladder

In order to meet the requirements of technical parameters, aramid fiber reinforced thermoplastic polyurethane polymer composite is used for the high-pressure flexible bladder. The assembly size is 2500 mm×2020 mm×100 mm, the thickness is 3 mm, and the corresponding actual working plane size is 2400 mm×1920 mm. The front of the flexible bladder is provided with a polyester woven reinforcement for protecting the skin. The support frame is connected to the outer side of the bladder in the circumferential direction. An oil inlet flange and an oil outlet flange are left on the back of the flexible bladder (see Fig.16). The thermoplastic polyurethane is clamped on the skin

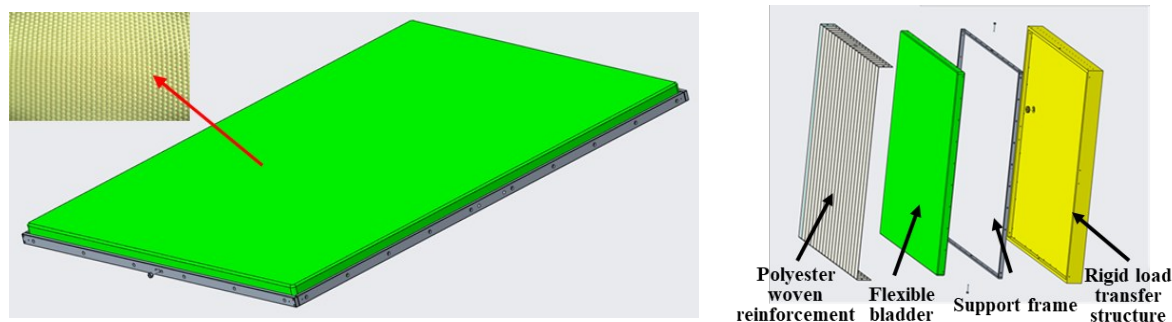


Fig.16 High-pressure flexible bladder

surface by the pre-tightening force of bolts, so that the skin surface is deformed and a tight sealing fit is realized.

2.3 Rigid load transfer structure

The rigid load transfer structure is used to transfer the concentrated load to the front high-pressure flexible bladder. The side and back of the rigid load transfer structure are connected with the support frame to wrap the main part of the bladder and provide it with lateral and forward constraints.

2.4 Liquid pressure sensor

The range of the liquid pressure sensor is 0–1.0 MPa, which is connected with the oil inlet and outlet flanges. The sensor transmits the pressure signal in the capsule to the servo control system to realize the pressure–displacement closed–loop control.

3 Test verification of uniform load application effect

3.1 Loading model

The box girder is selected from the bottom compartment of the hull, as shown in Fig.17. The main dimension of the box girder is 17000 mm×2400 mm×1200 mm, and the cross section and main dimensions are as shown in Fig.18. There are four L-shaped longitudinal stiffeners of 150 mm×50 mm×12 mm distributed on the deck and bottom plates, and three L-shaped longitudinal stiffeners of 150 mm×50 mm×12mm distributed on the side plate. In order to reduce the influence of the boundary, a 4-span range is taken vertically and 3 transverse frames are set inside. The thickness of the plates used in the effective test section is 6 mm while those in the transition section and the loading section are 20 mm, so as to ensure that the transition section and the loading section have sufficient strength to transfer the load.

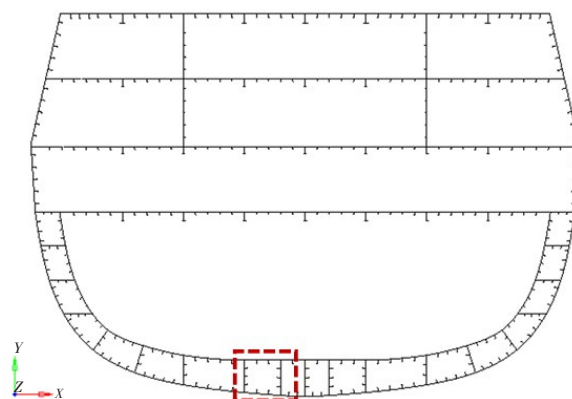


Fig.17 Model range of box girder structure

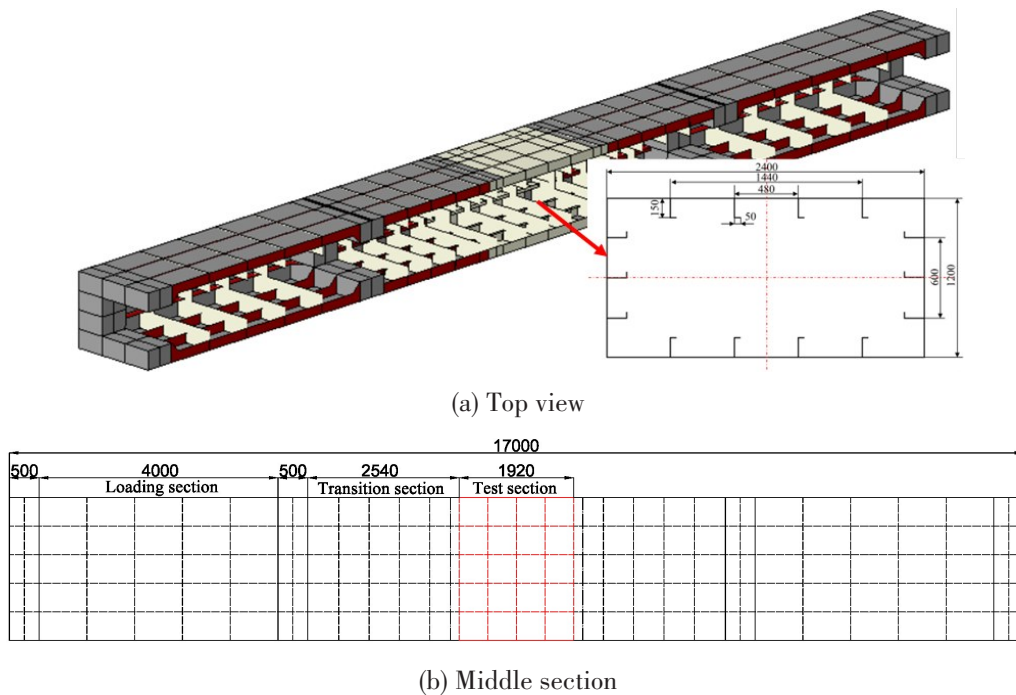


Fig.18 Structural diagram of box girder model (unit: mm)

3.2 Test scheme

In this experiment, combined loading of four-point bending moment and surface load is used to verify the effect of uniform load applied in the surface pressure loading system, as shown in Fig. 19. Before the test begins, the bladder is compressed after contact with the bottom plate. During the test, the 100 kPa surface pressure exerted by the surface pressure loading system is kept constant, and the bending moment load is provided by the 6000 kN hydraulic actuators on both sides, and the load is carried out in stages until the model is completely destroyed (see Fig.20).

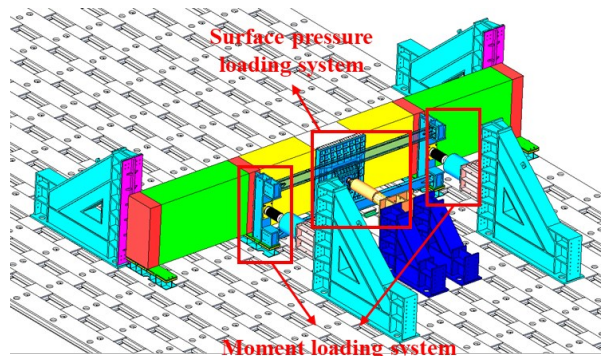


Fig.19 Ultimate strength test scheme for box girder



(a) Arrangement of ultimate strength test of box girder



(b) Four-point bending moment loading system



(c) Surface pressure loading system

Fig.20 Box girder ultimate strength test

20 triaxial strain gauges are uniformly arranged in the center of the bottom panel of the box girder to verify the uniform load effect of the system in Fig.21, and the von-Mises stress state of the panel center is obtained. The accuracy and reliability of the loading system are verified by comparing the measured values with the numerical results.

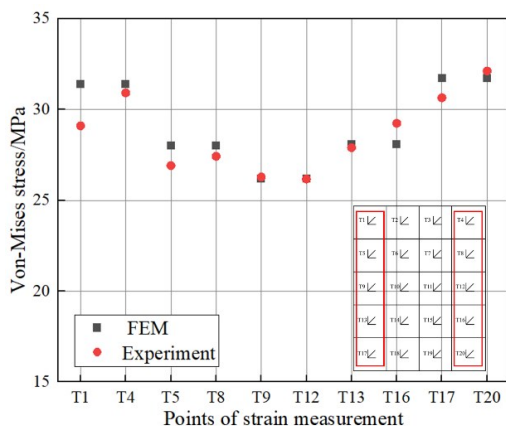
3.3 Effect of surface loading under different working conditions

3.3.1 Surface pressure loading of 100 kPa

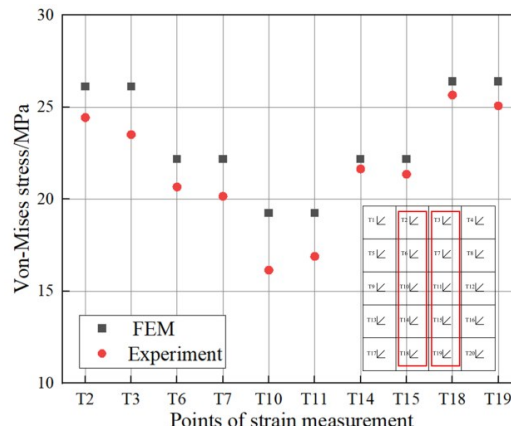
The pressure on the bottom plate of the box girder is gradually increased by squeezing the bladder by controlling the hydraulic actuator. When the pressure sensor of the bladder reaches 100 kPa, the von-Mises stress converted from the measured strain results (see Fig.22) is 0.05%–9.97% different from the numerical stress results (the deviation of T3 measuring point is 9.97%). It shows that the surface pressure loading system is accurate and reliable under the action of a single surface load.

T1 ↙	T2 ↙	T3 ↙	T4 ↙
T5 ↙	T6 ↙	T7 ↙	T8 ↙
T9 ↙	T10 ↙	T11 ↙	T12 ↙
T13 ↙	T14 ↙	T15 ↙	T16 ↙
T17 ↙	T18 ↙	T19 ↙	T20 ↙

Fig.21 Arrangement of strain gauges on the inner surface of box girder bottom plate



(a) Outer measuring points on the inner surface of the model bottom plate



(b) Inner measuring points on the inner surface of the model bottom plate

Fig.22 Stress comparison of measurement points on the inner surface of the model under a single surface pressure

3.3.2 Combined loading of surface pressure and bending moment loads

The surface stress of 100 kPa is maintained constant, and the bending moment load is gradual-

ly increased until the model fails. When the model reaches the ultimate state, the surface pressure load is reduced to 10 kPa to protect the bladder. During the test, the curve of the load applied by hydraulic actuator and surface pressure load–loading step is shown in Fig.23. The maximum deviation is 1.72%, indicating that the surface pressure loading system is accurate and reliable under the combined loads.

4 Conclusions

Aiming at the test requirements of uniform surface pressure loading in hull structure strength evaluation, a surface loading technology for ship structure test based on high–pressure flexible bladder was proposed, and a surface pressure loading system was developed. The following conclusions can be drawn:

(1) Using the loading mode of hydraulic actuator combined with high–pressure flexible bladder, the hydraulic actuator pushes the rigid load transfer structure, converting the concentrated load applied by the actuator into internal pressure of the bladder, and uniformly applying it to the surface of the ship structure. According to the numerical model of the loading device, the lateral pressure on the contact surface between the bladder and the hull is almost evenly distributed except for the high contact pressure on the outer edge of the bladder, which verifies the effectiveness of the loading device.

(2) The developed system is composed of a counter–force apparatus, a hydraulic actuator, a high–pressure flexible bladder (including a support frame), a rigid load transfer structure and a liquid pressure sensor. The surface pressure loading system has a loading area of 4.6 m² and a design load of 100 kPa. The skin of the flexible bladder is made of aramid–fiber reinforced thermoplastic polyurethane polymer composite material, which has high tensile strength (>167.0 MPa), corrosion resistance, oil resistance and wear resistance.

(3) Through the ultimate strength test of the box girder under the combined action of bending moment and surface pressure, the feasibility of the surface pressure loading system based on the high–pressure flexible bladder is verified systematically. The stress deviation of the measuring point under a single surface pressure is less than 10% compared with that in the ideal working condition. The maximum deviation of the surface pressure load under the combined action of bending moment and surface pressure is only 1.72%. The system realizes horizontal constant pressure loading with rapid load response and safe loading process, and the pressure load is always stable with the lifting of the bending moment load during the test. The system satisfies the requirement of uniform loading in the strength comprehensive test of large–scale structural models and improves the accuracy of the test results.

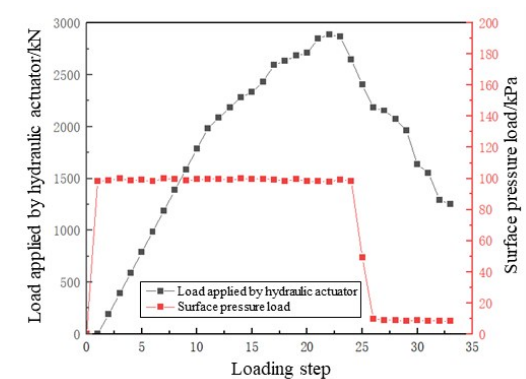


Fig.23 Load curves of combined loading

References

- [1] Guo S H, Guo T, Zhang Y, Cai C S. Experimental study on GFRP–Concrete combined bridge deck simple support slab[J].

- Journal of China & Foreign Highway, 2012, 32(04): 99–105.
- [2] Ma H Y, Xiong Q F, Wang D Y. Experimental and numerical study on the ultimate strength of stiffened plates subjected to combined biaxial compression and lateral loads[J]. Ocean Engineering, 2021, 228: 108928.
- [3] Zhuo Y, Lü Y B, Zhang W D. Research on tensile and compression pad loading technology in aircraft structural strength testing[J]. Science Technology and Engineering, 2016, 16(02): 244–248.
- [4] Shang H X, Wang H, He Y Z, et al. Simulation method of water load in structural strength test of amphibious aircraft[J]. Science Technology and Engineering, 2019, 19(14): 371–376.
- [5] Duan L G. The research and analysis of static test loading mechanism for the high-aspect ratio wing[D]. Yanshan: Yanshan University, 2015.
- [6] Pan T, Chen L, Fang Q, et al. Numerical testing analysis of quasi-static loading using airbag on reinforced concrete beam[J]. Research and Exploration in Laboratory, 2016, 35(04): 17–21+25. (in Chinese)
- [7] Chen S, Yang Z C, Li B. Design method of uniform loading system using airbags in structure test[J]. Engineering Mechanics, 2012, 29(06): 146–150. (in Chinese)
- [8] Wang Z, Zhang J F, Liu B. Research and application of airbag loading in static testing of aircraft structures[J]. Manufacture and Upgrading Today, 2020(10): 99–100. (in Chinese)
- [9] Yang P F, Fu M S, Xia F. Research and application of negative pressure loading technology for aircraft fuel tank lower wall [J]. Engineering and Test, 2019, 59(04): 72–73. (in Chinese)
- [10] Padalu P K V R, Singh T, Das S. Cyclic two-way out-of-plane testing of unreinforced masonry walls retrofitted using composite materials[J]. Construction and Building Materials, 2020, 238: 117784.
- [11] Shanmugam N E, Zhu D Q, Choo Y S, et al. Experimental studies on stiffened plates under in-plane load and lateral pressure[J]. Thin-Walled Structures, 2014, 80: 22–31.

船舶结构表面载荷加载技术研究

戴泽宇^{1,2}, 韦朋余^{1,2}, 陈小平^{1,2}, 蒋 泽^{1,2}, 陈 哲^{1,2}, 唐 沁³

(1. 中国船舶科学研究中心, 江苏 无锡 214082; 2. 深海技术科学太湖实验室, 江苏 无锡 214082;

3. 江南大学 外国语学院, 江苏 无锡 214122)

摘要:表面压力载荷易引起船体结构局部变形和损伤,如何模拟表面载荷加载一直是船舶结构试验技术领域亟待解决的问题。本文提出“液压作动器+高压柔性液囊”的加载模式,建立加载装置数值模型,形成基于芳纶纤维增强热塑性聚氨酯的高压柔性液囊结构设计与分析方法,突破船舶结构表面载荷加载技术,研制一种基于高压柔性液囊的表面载荷加载系统,并开展弯矩和表面压力联合作用下箱型梁模型极限强度验证试验,系统验证加载系统的可行性和适用性。结果表明,采用表面载荷加载技术能对船体结构较好地施加均匀布压力,相较于传统重物堆载法,该方法可实现卧式恒压力全自动加载,载荷响应迅速,加载过程安全,且试验过程中随着弯矩载荷的提升表面压力载荷始终稳定,可很好地满足大尺度结构模型强度综合试验均布载荷加载的要求,提高试验结果的准确性。

关键词:表面载荷; 加载系统; 船舶结构; 强度试验; 柔性液囊

中图分类号: U661.1 **文献标识码:** A

基金项目: 国家重点研发计划资助项目(2022YFB3404800)

作者简介: 戴泽宇(1995-),男,中国船舶科学研究中心工程师;
韦朋余(1982-),男,中国船舶科学研究中心研究员;
陈小平(1983-),男,中国船舶科学研究中心高级工程师;
蒋 泽(1995-),男,中国船舶科学研究中心工程师;
陈 哲(1987-),男,中国船舶科学研究中心工程师;
唐 沁(1985-),女,江南大学外国语学院副教授。